Modeling and Prediction of Land Use and Land Cover Change Dynamics Using Markov Model in Jodhpur Tehsil,Rajasthan, India

Ankita Pandey[1]* Dr. Khundrakpam Moirangleima[2]

Abstract

Land Use and Land Cover (LULC) change analysis offers crucial insights into the spatial dynamics influenced by human and environmental interactions. This study examines LULC transitions in Jodhpur Tehsil, Rajasthan, India, from 1993 to 2023. It predicts future patterns for 2033 using the Cellular Automata–Markov (CA– Markov) model in the TerrSet Geospatial Monitoring and Modeling System. Multi-temporal Landsat imagery (1993, 2003, 2013, and 2023) was classified into five major categories—agriculture, barren land, built-up areas, mining, and water bodies—through supervised Maximum Likelihood Classification.

Accuracy assessment achieved an overall accuracy of 85–88% and Kappa coefficients above 0.80, validating the classification reliability. Results indicate a continuous decline in agricultural land (73.40% to 62.87%) and expansion of built-up (6.17% to 16.33%) and mining areas (0.48% to 1.70%) over three decades. The Markov transition probability matrix predicts further conversion of agricultural and barren lands into built-up and mining zones by 2033. Model validation confirmed strong spatial agreement between predicted and actual LULC maps.

The study highlights significant anthropogenic pressure on land resources and demonstrates the CA–Markov model's efficiency for simulating future LULC dynamics, offering valuable guidance for sustainable land management and urban planning in arid regions.

Keywords: LULC Prediction, CA – Markov Model, Spatial Simulation, Land Transformation, Future Land Dynamics

Introduction

Over the last few decades, Land Use and Land Cover (LULC) change has emerged as one of the central issues in environmental research, largely because it directly influences ecosystem functioning, water availability, and climate regulation [1,2]. These changes are not isolated events but are the cumulative result of anthropogenic pressures such as agriculture, mining, and rapid urban growth, combined with natural drivers like climate variability and soil degradation [1,3]. At the global scale, shifts in land cover reflect trade-offs between economic development and environmental sustainability, with consequences ranging from biodiversity decline to alterations in the carbon cycle [3,4]. This makes the study of LULC change vital for guiding sustainable land management practices across diverse geographies. [1,2].

The dynamics of LULC are particularly complex because they operate across multiple spatial and temporal scales, producing both immediate and long-term transformations [2,4]. For instance, while agricultural intensification can provide short-term food security, it often accelerates deforestation and land degradation in the long run [3]. Similarly, urban expansion in Asia and Africa has been identified as a dominant factor reshaping peri-urban and rural landscapes [3,5]. Mining further amplifies these pressures, as it replaces natural or agricultural land covers with extraction sites and waste dumps, producing permanent landscape scars and driving socio-ecological vulnerabilities [3,6]. Such

[1] Research Scholar School of Earth Sciences, Banasthali Vidyapith, Rajasthan – 304002, India Email: malitoankita1997@gmail.com

[2]Associate Professor School of Earth Sciences, Banasthali Vidyapith, Rajasthan – 304002, India Email: mkhundrakpam@banasthali.in

examples highlight why predictive modeling of LULC change is necessary, especially in regions where economic development is closely tied to resource extraction. [4,5].
Globally, predictive modeling of mining-related LULC change has been successfully applied. 3,6]. In Brazil, CA–Markov modeling revealed extensive forest loss due to iron ore extraction, underlining long-term biodiversity threats [4,7]. In China, similar approaches demonstrated how coal mining triggered rapid conversion of farmland into degraded wastelands, influencing food security and water dynamics [3]. In India, studies in Goa, Odisha, and Jharkhand have highlighted how bauxite, iron, and coal mining have driven forest fragmentation and agricultural decline, threatening local [3,8]. These studies illustrate the value of predictive approaches in anticipating mining-driven land cover transitions.
Over the years, a wide range of models have been employed for simulating LULC dynamics, each with unique strengths and limitations [1,2] . Statistical models such as logistic regression and generalised linear models are widely used for identifying the relationship between driving forces and land cover [4]. Agent-based models simulate the decision-making behavior of individuals or institutions, making them suitable for socio-economic driven changes [2]. Machine learning approaches, including random forests and neural networks, have gained popularity for handling complex, non-linear. However, one of the most widely applied frameworks remains the combination of Markov chains with Cellular Automata (CA–Markov), which merges stochastic transition probability estimation with spatial neighborhood effects [5,9].
The Markov model in particular is praised for its ability to estimate transition probabilities of land cover classes based on past temporal sequences, making it especially valuable in identifying long-term trends [4]. When integrated with cellular automata, the CA–Markov framework enhances spatial realism by incorporating neighborhood rules, thus bridging statistical prediction with spatial simulation [5,9]. Several studies have shown that the CA–Markov model performs better than standalone statistical or machine learning models when predicting gradual and spatially explicit changes, such as those driven by urbanization and [5,11]. Its flexibility, transparency, and proven track record make it one of the most reliable tools for regional LULC prediction.
The Jodhpur region of Rajasthan, India, presents a particularly relevant case for such research also known as the “Sun City,”. Jodhpur is simultaneously a hub for cultural heritage and mining activity, with sandstone, limestone, and granite extraction shaping its land cover for decades [12,13]. Mining has contributed significantly to regional economic growth but has also intensified challenges such as land degradation, groundwater depletion, and habitat destruction .Between 1993 and 2023, satellite-based LULC analysis from USGS imagery has revealed noticeable increases in mining land and built-up areas, accompanied by losses in scrubland and agricultural land .These trends raise concerns for sustainable land and water management in the arid ecosystem of Jodhpur tehsil [14,15].
In this study, the CA–Markov model is applied to simulate future LULC transitions, building on its demonstrated success in predicting complex land use patterns [5, 9,11]. By combining the stochastic strengths of Markov chains with the spatial allocation of cellular automata, the model offers robust predictive capacity for mining landscapes [4,9] . Assessing future scenarios is crucial because unregulated mining expansion could lead to irreversible transformations, including accelerated desertification, groundwater stress, and reduced agricultural productivity [2,14]. Thus, understanding and predicting mining-induced LULC dynamics in Jodhpur is not only a scientific exercise but also a step toward informed land-use policies, sustainable mining practices, and long-term ecological resilience. [2,6,12].

2. Materials and Methods

2.1. Study Area

Jodhpur Tehsil, located in the western part of Rajasthan, India, forms the core administrative and economic hub of Jodhpur district. Geographically, it lies between **26°00′ to 27°00′ N latitude and 72°30′ to 73°30′ E longitude**, covering an area of approximately **6,000 km²** as shown in **Table 1** . The region is part of the arid and semi-arid landscape of the Thar Desert, characterized by extreme climatic conditions, including high summer temperatures (often exceeding 45°C) and low annual

rainfall averaging around 350 mm . Such environmental settings make land and water resources highly vulnerable to anthropogenic pressures.

Economically, Jodhpur Tehsil is well known for its **sandstone, granite, and limestone mining**, which has been a cornerstone of regional development for decades and also Jodhpur is also known as the **"Sun City"**, famous for its heritage architecture and tourism. However, the unchecked growth of mining and urbanization is creating new challenges in terms of **land degradation, desertification risks, and groundwater stress**.

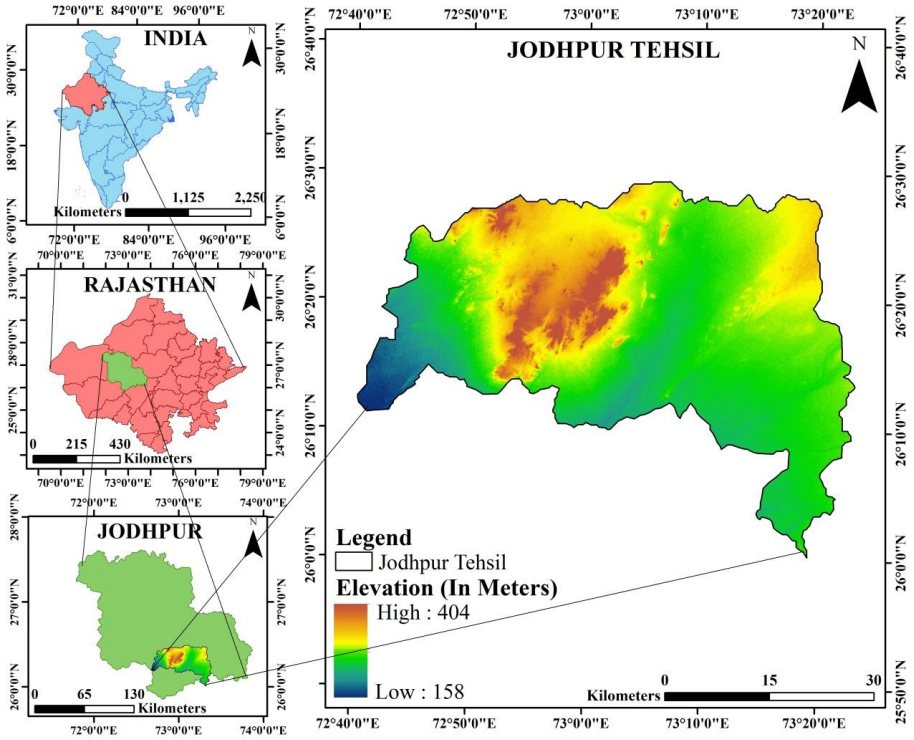

Figure 1 The Study area

2.2. Data Types and Sources

The study utilised multi-temporal remotely sensed satellite imagery to analyze and predict the spatio-temporal dynamics of land use and land cover (LULC) changes in Jodhpur Tehsil, Rajasthan, India. Landsat images were obtained from the United States Geological Survey (USGS) Earth Explorer platform(https://earthexplorer.usgs.gov/), corresponding to Path 149/Row 042. Four temporal datasets—1993, 2003, 2013, and 2023—were selected to capture decadal transitions in LULC patterns associated with the expansion of sandstone mining and related anthropogenic activities.

The Landsat 4–5 TM image from 1993 served as the baseline to represent the early phase of mining operations and to establish the initial LULC classification. The Landsat 7 ETM+ image from 2003 facilitated the assessment of intermediate changes, particularly the emergence and intensification of mining zones. The Landsat 8 OLI/TIRS image from 2013 captured further spatial modifications, including the progression of mining areas and corresponding transformations in vegetation and built-up regions. Finally, the Landsat 8–9 OLI image from 2023 provided the most recent data, allowing evaluation of the current extent of mining activities, settlement growth, and environmental alterations.

In addition to the temporal imagery, several spatial variables were also processed to enhance the understanding of factors influencing land transformations. Road density was derived from OpenStreetMap (OSM) data, obtained through the BBBike portal. Mine density and built-up density were extracted from the classified LULC maps of Jodhpur Tehsil for respective years. Elevation and slope data were generated from a Digital Elevation Model (DEM) at 30 m spatial resolution, enabling the assessment of topographic influences on land use changes. **Table. 1** illustrates the details of gathered data.

Satellite/Sensor / Data Source	Path/Row	Bands / Variables	Spatial Resolution	Source
Landsat 4–5 TM (1993)	149/042	1–5, 7	30 m	USGS Earth Explorer (https://earthexplorer.usgs.gov/)
Landsat 7 ETM+ (2003)	149/042	1–5, 7, 8	30 m	USGS Earth Explorer (https://earthexplorer.usgs.gov/)
Landsat 8 OLI/TIRS (2013 & 2023)	149/042	1–7, 9	30 m	USGS Earth Explorer (https://earthexplorer.usgs.gov/)
OpenStreetMap (OSM) – Road Network	-	Road (Polyline)	(~10 m accuracy)	BBBike Portal (https://extract.bbbike.org/)
SRTM Digital Elevation Model (DEM)	-	Elevation	30 m	USGS Earth Explorer (https://earthexplorer.usgs.gov/)

Table 1 Datasets and their sources

2.3 Methodology

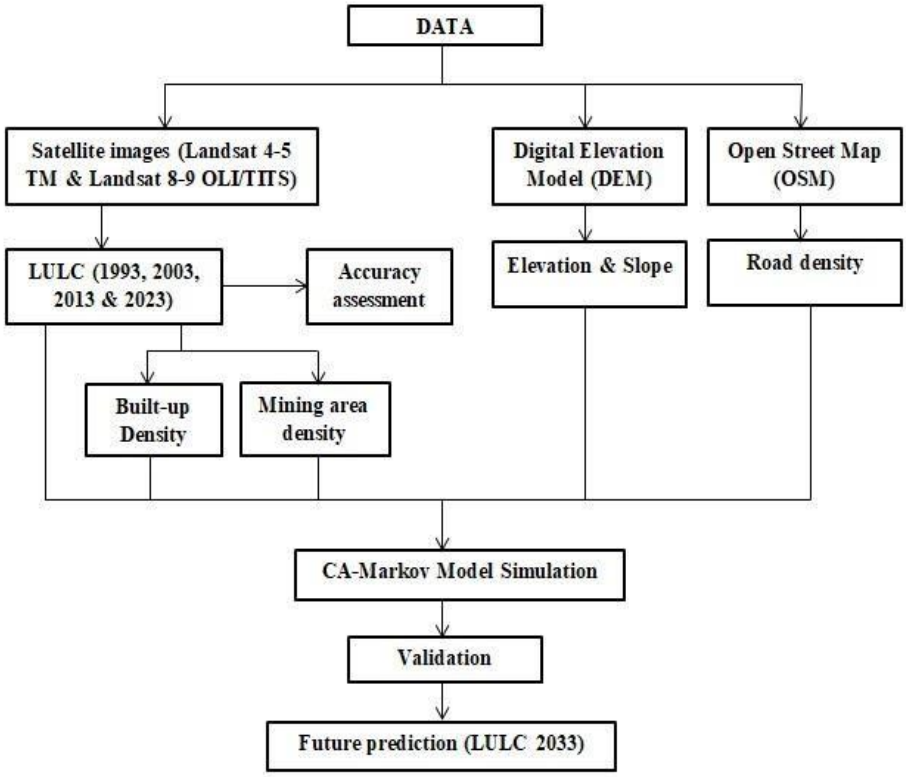

Figure 2 The Methodology Flow Chart

The methodological framework adopted in this study is illustrated in **Fig. 2** which integrates remote sensing, GIS, and spatial simulation modelling to analyse and predict Land Use and Land Cover (LULC) changes in Jodhpur Tehsil. Multi-temporal Landsat datasets were processed, classified, validated, and subsequently modelled using the CA–Markov approach implemented in TerrSet. This framework enables the assessment of past land dynamics and the projection of future land-use scenarios in a spatially explicit manner [17,18].

2.3.1. Image Classification

Image classification plays a central role in LULC analysis by converting spectral information into meaningful thematic classes. Landsat images from 1993, 2003, 2013, and 2023 were classified to evaluate temporal land-use dynamics. Standard pre-processing procedures, including geometric correction and atmospheric normalization, were applied to ensure consistency across time periods [19].

A supervised Maximum Likelihood Classification (MLC) algorithm was employed due to its statistical robustness and widespread use in LULC studies. Training samples were selected using ground truth observations, Google Earth imagery, and historical reference data. The classification scheme comprised five distinct LULC categories as shown in **Table 2** , representing the dominant land use patterns in the region.

LULC Type	Description
Mining	Includes active sandstone quarries, mining pits, waste dumps, and associated extraction zones.
Agriculture	Areas under seasonal or perennial cultivation, croplands, and fallow lands used for farming activities.
Barren Land	Exposed rocky surfaces, degraded land, and uncultivated areas with minimal vegetation cover.
Built-up	Urban settlements, rural habitations, roads, and infrastructure development zones.
Water Body	Rivers, ponds, reservoirs, and other permanent or seasonal water sources.

Table 2 LULC classes and their description in accordance with study area

2.3.2. Accuracy Assessment

To evaluate the reliability of the classified LULC maps, an accuracy assessment was performed using reference data. A total of 50 sample points per class were systematically selected and verified using high-resolution realworld imagery. These points were then used to extract corresponding LULC class values from the classified maps through the Extract Multi Values to Points tool in ArcGIS.

The extracted values were organized into a frequency table, which was subsequently used to generate a pivot table (also known as an error matrix or confusion matrix). This matrix facilitated the computation of key accuracy metrics, including User's Accuracy (UA), Producer's Accuracy (PA), Overall Accuracy (OA), and the Kappa Coefficient (κ), as defined in **equations 1,2,3 and 4** respectively, following standard statistical procedures.

The formulas applied for the evaluation are as follows:

$$\text{1. Overall Accuracy (OA)} = \frac{\Sigma \text{ Correctly classified samples}}{\text{Total number of samples}} \times 100 \quad (1)$$

$$\text{2. Producer's Accuracy (PA)} = \frac{\text{Correctly classified pixels in a class}}{\text{Total reference pixels in that class}} \times 100 \quad (2)$$

$$\text{3. User's Accuracy (UA)} = \frac{\text{Correctly classified pixels in a class}}{\text{Total classified pixels in that class}} \times 100 \quad (3)$$

$$\text{4. Kappa Coefficient (κ)} = \frac{N \times \Sigma xii \; - \Sigma(xi+ \; \times x+i \;)}{N^2 - \Sigma(xi+ \; \times x+i \;)} \quad (4)$$

where:

N = total number of samples xii = correctly classified samples in class i xi+ = total reference samples in class i (row total) x+i = total classified samples in class i (column total)

2.3.3 Preparation of Spatial Variables

In order to support the spatial modelling, key explanatory variables had been derived. A 30m Digital Elevation Model(DEM) was incorporated for the elevation data from which the slope was generated

after projecting it to a consistent coordinate system. The density layers of Built-up and mining areas were obtained from the classified LULC maps by extracting relevant classes, convention them into vector format and then generating the density surfaces by using the point density analysis. The road density was calculated by incorporating the line density tool with the OpenStreetMap road network. The resulting variables, such as elevation, slope, Built-up, mining and road density, served as primary inputs for subsequent modelling and analysis. **Fig. 3** depicts the various spatial variables used in LULC prediction

2.3.4 Input Preparation for Model

All the spatial variables, including the LULC layers, were resampled to a uniform 30m resolution to ensure consistency. The standardisation of the rows, columns and projections had to be done across all the datasheets to maintain the homogeneity in the cell size and for the spatial alignment. To ensure compatibility and spatial accuracy, each variable had to be projected to UTM Zone 43. Therefore, all the datasheets were converted into .rst format to become compatible with the TerrSet modelling environment.

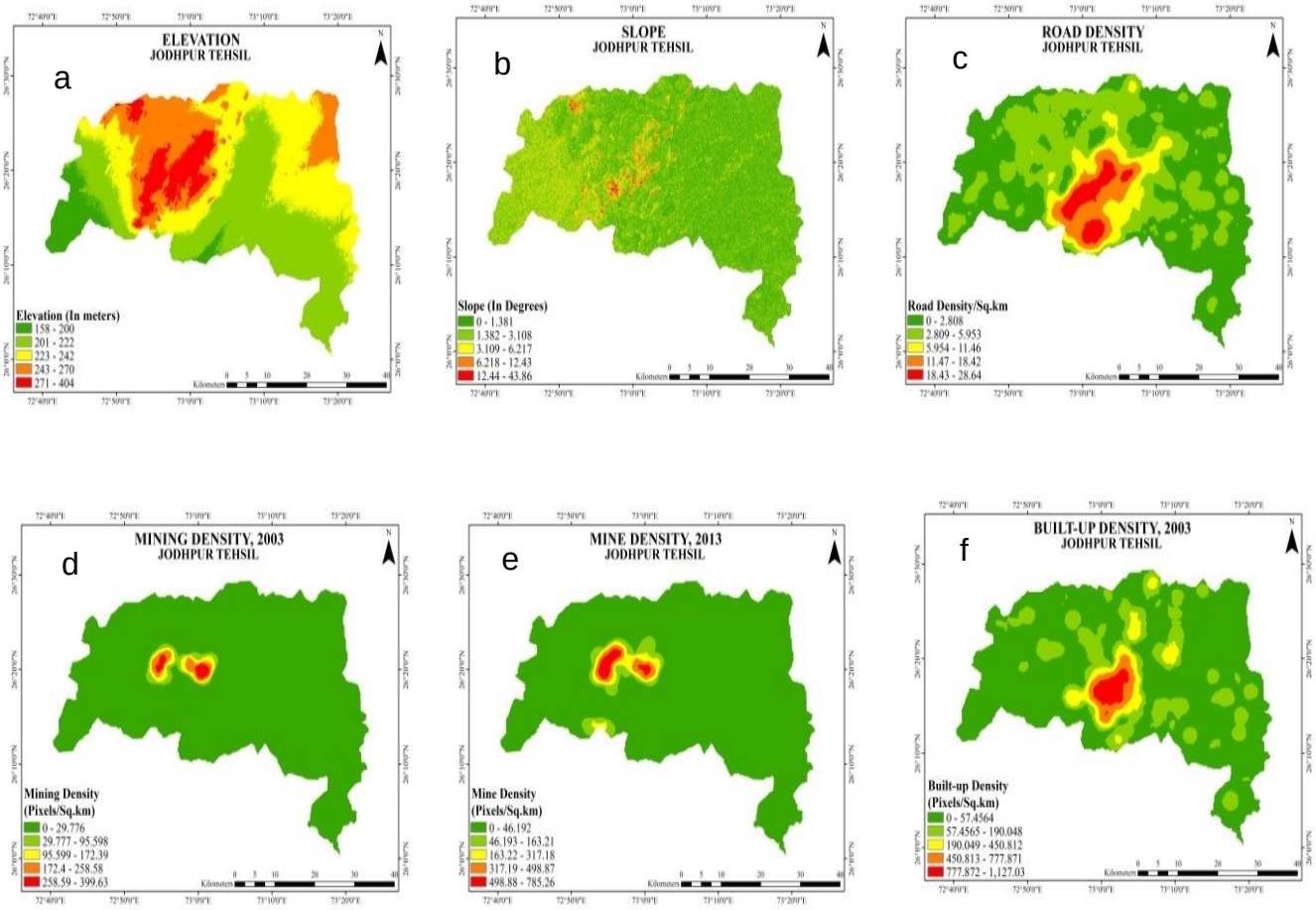

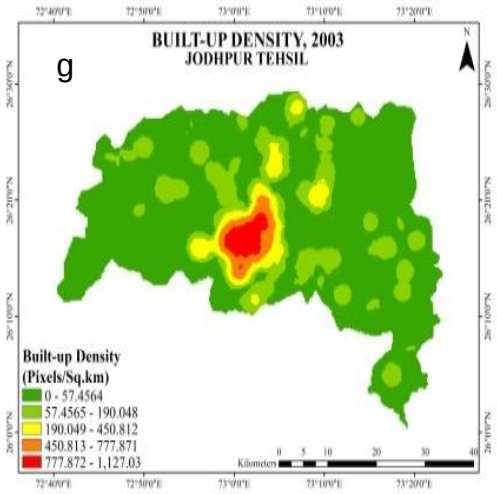

Fig. 3 Important spatial variables which effect LULC change in JodhpurTehsil. (a) elevation, (b) slope, (c) roaddensity, (d) mining area density-2013, (e) mining area density-2023, (f) built-up density-2013 and (g) built-updensity-2023).

2.3.5 Markov Model Simulation

The CA-MARKOV model used in TerrSet 2020 was incorporated to simulate and predict the future Land Use and Land Cover (LULC) changes in the Jodhpur Tehsil. In order to generate temporally consistent and spatially accurate LULC projections, the Markov chain-based transition probabilities were integrated with the Cellular Automata spatial rules. All LULC maps and driving variables had to be standardised and converted into .rst format to ensure uniform projections, resolution and cell size.

The simulations were done with the Land Change Modeller(LCM) module. The historical LULC transitions had to be validated via the Change Analysis component, whereas the suitability maps had to be generated in the Transition Potential module by incorporating spatial drivers such as elevation, slope, road, built up and mining densities. The Markov Chain module was used to derive the transition probability matrices. The 2003 LULC map was used to predict 2013, 2013 to forecast 2033 and 2023 to generate a subsequent 2033 scenario. The Cellular Automata neighbourhood rules were applied to spatially allocate the predicted changes and forecast future LULC maps.

This integrated framework proves to be highly effective in determining both spatial and temporal LULC dynamics, thus providing a reliable basis for assessing the mining and urban expansion by supporting the sustainable land use planning in Jodhpur Tehsil.

2.4. LULC Change Prediction and Validation

2.4.1. LULC Prediction

Predictions of Land Use and Land Cover (LULC) dynamics is highly important for sustainable land management and environmental planning. In this study, future LULC scenarios for Jodhpur Tehsil were simulated using the Land Change Modeller (LCM) in the TerrSet Geospatial Monitoring and Modelling System, which is based in classified satellite images from 1993,2003,2013 and 2033 . The LCM model analyses the historical data of land cover transitions, evaluates the driving factors and then generates a transition probability matrices to estimate the future land cover [17,20].

The model gives two outputs: hard prediction maps by assigning each pixel to a specific LULC class and soft prediction maps by representing vulnerability to change on a continuous scale from 0-1, where the higher values indicate greater susceptibility [17]. The LCM workflow comprises of three modules: Change Analysis, Transition Potential and Change Prediction. The Change Analysis refers to the transition rates from 1993-2003, 2003-2013 & 2013-2023. The factors incorporated in generating the transition maps were elevation, slope, proximity to roads and existing land cover as explanatory variables, followed by simulation of future scenarios. [21].

Multi- Layer Perceptron (MLP) neural network was incorporated for generating transition potentials as this effectively analyses the nonlinear relationship between LULC change and the driving factors which results in higher predictive accuracy [21] as presented in equation 5,6 and 7. The integrated Cellular Automata -Markov Chain (CA-MC) approach, was used for the spatial allocation of changes. The Markov Chain estimates transition probabilities based on past changes and is expressed as:

$$S(t+1)=PijS(t) \quad (5)$$

Where, S(t) and S(t+1) represent land cover states at times t and t+1, and Pij is the transition probability matrix:

$$Pij = \begin{matrix} P11 & P12 & \cdots & P1n \\ P21 & P22 & \cdots & P2n \\ \vdots & \vdots & \ddots & \vdots \\ Pn1 & Pn2 & \cdots & Pnn \end{matrix} \quad (6)$$

$$0 < Pij < 1, \ \Sigma n \ j = 1 \ Pij = 1$$

The Cellular Automata component allocates these transitions spatially by incorporating neighborhood effects, defined as:

$$S(t,t+1)=f[S(t),N] \quad (7)$$

Where, 'N' represents neighbourhood influence and 'f'denotes local transition rules. The CA–Markov model thus integrates stochastic transition probabilities with spatial neighbourhood dynamics to generate realistic LULC projections, supporting land-use planning and environmental management in semi-arid regions.

2.4.2. Model Validation

Model validation was performed to assess the reliability of predicted LULC maps .Initially, LULC maps from 1993 and 2003 were used to predict the 2013 LULC map, which was compared with the actual 2013 classification. Subsequently, the 2003–2013 dataset was used to predict the 2023 LULC map and validated against observed 2023 data, capturing significant mining-related changes. After satisfactory validation, the 2013–2023 dataset was used to predict the 2033 scenario. [24].

The Kappa statistics was used to authenticate the validation assessed hits, false alarms, misses and the agreement between predicted and observed maps. In order to overcome the limitations of Kappa Coefficient, advanced variants had to incorporated which includes the Kappa for no information (Kno), Kappa for location (Klocation), Kappa for standard (Kstandard) and Kappa for stratum-level location (KlocationStrata) [24]. These matrics distinguish quantity disagreement from spatial allocation disagreement. In order to analyse the source of prediction error seveal other factors were analysed such as Agreement Quantity, Agreement Grid Cell, Disagreement Quantity and Disagreement Grid Cell [20]. The Kappa values ranging from 0.61-0.80 indicates substantial agreement whereas values above 0.81 indicates likely perfect agreement [26].

The definitive agreement between predicted and observed LULC maps for 2013 and 2023 validates the robustness of the LCM-CA-Markov framework, thus providing certainty in the future LULC projections and their application for the sustainable land use planning in Jodhpur Tehsil.

3. Results and Discussions

3.1. Accuracy Assessment of the Classified Images

Accuracy assessment ensured the reliability of the LULC classification using an error matrix to derive Producer's Accuracy (PA), User's Accuracy (UA), Overall Accuracy, and the Kappa Coefficient. As shown in **Table 3**, overall accuracy remained high for 1993 (88%), 2003 (88%), 2013 (85%), and 2023 (88%), with Kappa values between 0.81 and 0.85, indicating strong agreement with reference data. Water and built-up classes achieved the highest PA and UA, while barren land showed relatively lower accuracy due to spectral overlap. The consistently high accuracy across all years confirms the robustness of the classification and the reliability of the LULC results over time.

Accuracy assessment of land use land cover								
	1993		2003		2013		2023	
	PA %	UA %	PA %	UA %	PA %	UA %	PA %	UA %
Water	90	96.42	80	100	80	96	90	96.42
Agriculture	86.66	81.25	93.33	87.5	86.66	83.87	90	84.37
Mining	86.66	100	90	93.10	80	85.71	83.33	96.15
Built-up	93.33	93.33	90	93.10	93.33	87.5	83.33	86.20
Barren land	83.33	73.52	86.66	72.22	86.66	76.47	93.33	80
Overall accuracy (%)	88		88		85		88	
Kappa Coefficient	0.85		0.85		0.81		0.85	
PA= Producer's Accuracy UA=User's Accuracy								

Table 3 Accuracy statistics of LULC (1993-2023)

3.2 LULC Analysis

Area of LULC classes								
	1993		2003		2013		2023	
	Sq.km	Percent	Sq.km	Percent	Sq.km	Percent	Sq.km	Percent
Agriculture	1467.45	73.40	1467.97	73.43	1378.71	68.97	1256.84	62.87
Barren Land	386.34	19.32	374.66	18.74	347.46	17.38	365.59	18.29
Built Up	123.31	6.17	131.59	6.58	225.27	11.27	326.46	16.33
Mining Area	9.56	0.48	11.61	0.58	32.89	1.65	34.03	1.70
Water Body	12.55	0.63	13.37	0.67	14.76	0.74	16.17	0.81
TOTAL	1999.21	100.00	1999.20	100.00	1999.10	100.00	1999.10	100.00

Table 4 Area under each LULC class (1993-2023)

As illustrated in **Fig. 4**, the LULC maps for 1993, 2003, 2013, and 2023 clearly depict both spatial and temporal shifts in land cover patterns. Built-up areas show a continuous expansion throughout the study period. Mining activity initially expanded but later stabilized, indicating a transition toward a more constant trend. Conversely, agricultural land has steadily declined, reflecting on-going land conversion pressures in the region. The spatial–temporal analysis of LULC from 1993 to 2023 is shown **Table 4** which shows marked landscape changes. In 1993, agriculture dominated the area with 1467.45 sq. km (73.40%), followed by barren land (386.34 sq. km; 19.32%), built-up (123.31 sq. km; 6.17%), mining (9.56 sq. km; 0.48%), and water bodies (12.55 sq. km; 0.63%).

By 2023, agricultural land declined to 1256.84 sq. km (62.87%), indicating substantial conversion to other uses, while barren land showed minor fluctuations, reaching 18.29%. In contrast, built-up areas expanded sharply from 6.17% to 16.33%, and mining areas increased from 0.48% to 1.70%, reflecting urban growth and intensified resource extraction. Water bodies showed a slight increase to 0.81%. Overall, the results indicate a clear shift from agricultural land toward urban and mining uses, highlighting increasing anthropogenic pressure and the need for sustainable land management.

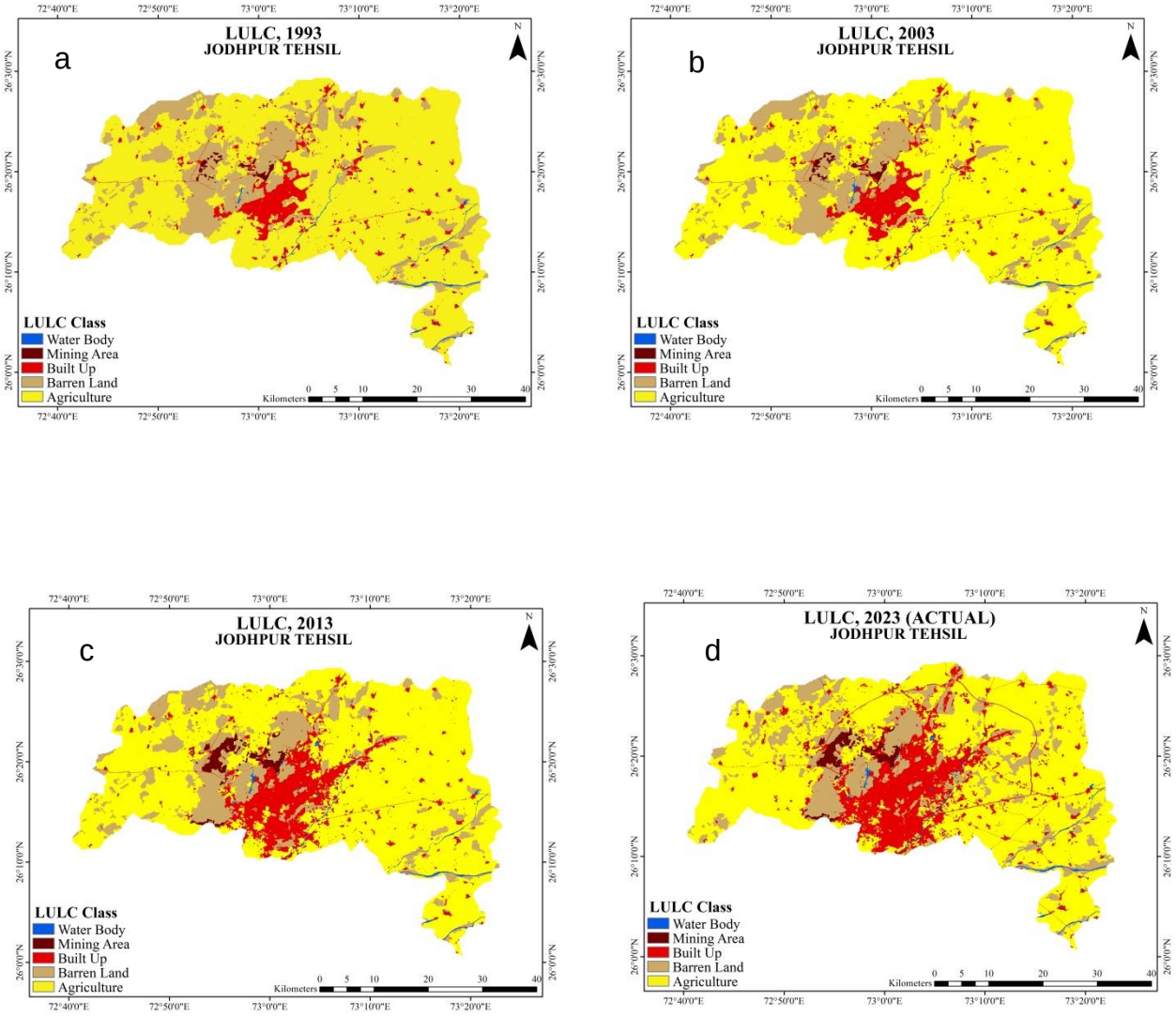

Figure 4: Land Use Land Cover maps, (a) LULC 1993, (b) LULC 2003, (c) LULC 2013 and (d) LULC 2023

3.3 Change Analysis

	1993-2003		2003-2013		2013-2023		2023-2033	
	Sq.km	**Percent**	**Sq.km**	**Percent**	**Sq.km**	**Percent**	**Sq.km**	**Percent**
Agriculture	0.52	0.03	-89.26	-4.46	-121.88	-6.10	1.05	0.06
Barren Land	-11.68	-0.58	-27.19	-1.36	18.13	0.91	-95.05	-4.73
Built Up	8.29	0.41	93.68	4.69	101.19	5.06	1.09	0.07
Mining Area	2.05	0.10	21.28	1.06	1.14	0.06	91.62	4.61
Water Body	0.81	0.04	1.39	0.07	1.42	0.07	0.31	0.03

Table 5 Decadal change/gain and loss in area of each LULC class (1993-2033)

As **Table 5** shows, the decadal change analysis from 1993 to 2033 highlights a clear shift in land-use dynamics across the region. Built-up areas consistently expanded, especially during 2003-2013 and 2013–2023, reflecting rapid urban growth. Agricultural land declined notably during the same periods, indicating steady conversion to urban and mining uses. Mining activity showed sharp increases in 2003–2013 and again in the projected 2023– 2033 decade, driven by intensified resource extraction. In contrast, barren land and water bodies exhibited only minor fluctuations, suggesting more localized and less intensive changes. The gain–loss and net-change graphs in **Fig. 5** clearly illustrate the magnitude and direction of land cover transitions across the three study periods. Built-up areas show the highest and most consistent gains, particularly during 2003–2013 and 2013–2023, reflecting accelerated urban expansion. Agriculture exhibits substantial losses, especially after 2013, indicating large-scale conversion to built-up and barren categories. Mining displays notable gains during 2003–2013, followed by modest increases thereafter. Barren land shows fluctuating gains and losses, highlighting localized degradation and reclamation dynamics over time.

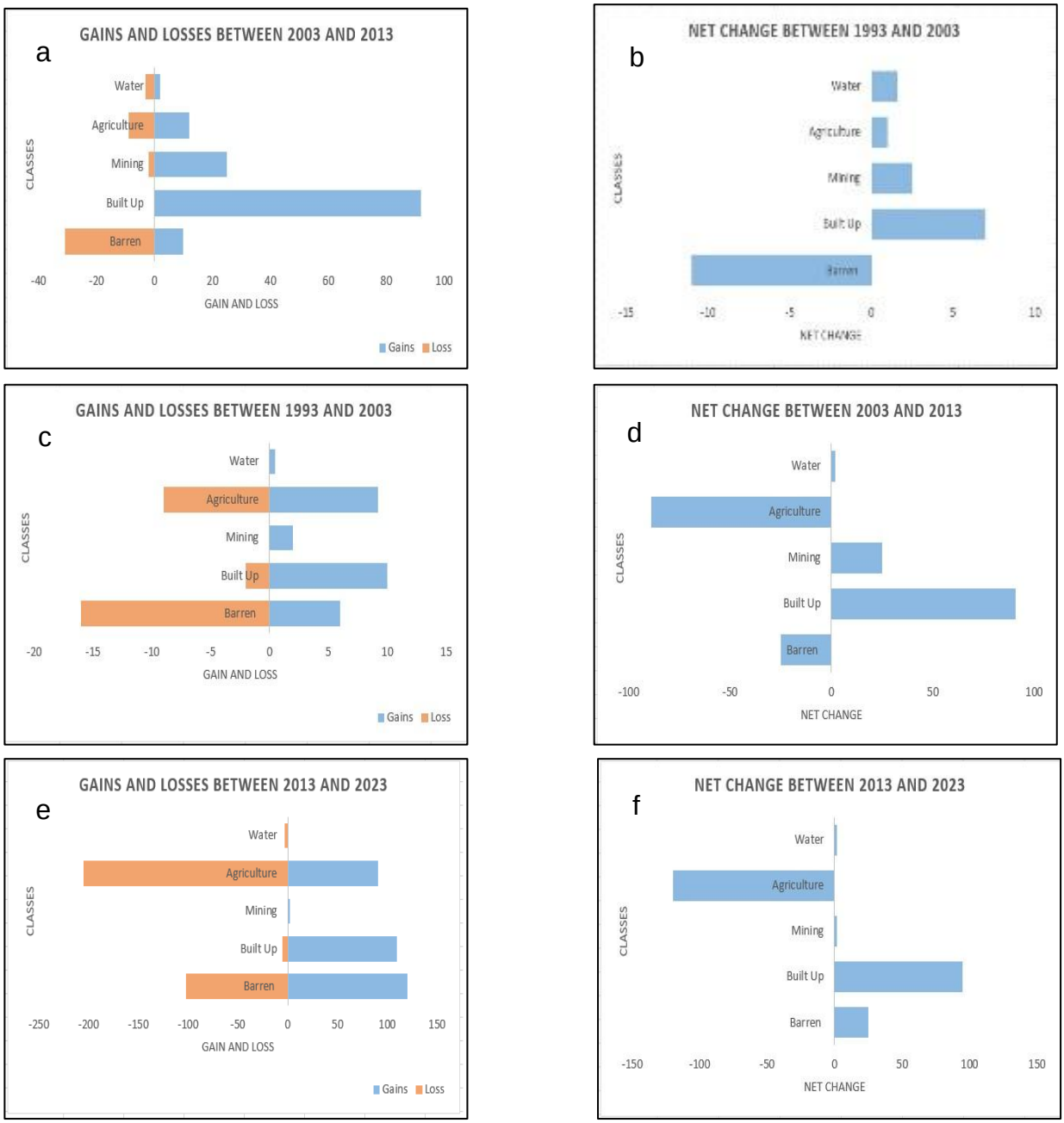

Figure 5 Change in LULC area, (a) gain and loss during 1993-2003, (b) net change during 1993-2003, (c) gainand loss during 2003-2013, (d) net change during 2003-2013, (e) gain and loss during 2013-2023 and (f) netchange during 2013-2023

Change detection 1993-2003							
LULC classes		2003					
		Agriculture	Barren Land	Built Up	Mining Area	Water Body	Grand Total
1993	Agriculture	1458.58	4.84	3.40	0.00	0.63	**1467.45**
	Barren Land	7.87	369.73	6.55	2.06	0.14	**386.34**
	Built Up	1.52	0.09	121.64	0.00	0.05	**123.31**
	Mining Area	0.00	0.01	0.00	9.55	0.00	**9.56**
	Water Body	0.01	0.00	0.00	0.00	12.55	**12.55**
	Grand Total	**1467.98**	**374.66**	**131.59**	**11.61**	**13.37**	**1999.21**

Table 6 Change detection/transition analysis (1993-2003)

Change detection 2003-2013							
LULC classes		2013					
		Agriculture	Barren Land	Built Up	Mining Area	Water Body	Grand Total
2003	Agriculture	1367.67	8.96	88.95	0.94	1.45	**1467.97**
	Barren Land	10.87	338.22	4.55	21.01	0.01	**374.66**
	Built Up	0.03	0.01	131.55	0.00	0.00	**131.59**
	Mining Area	0.20	0.29	0.16	10.94	0.03	**11.61**
	Water Body	0.02	0.01	0.07	0.00	13.28	**13.37**
	Grand Total	**1378.79**	**347.49**	**225.27**	**32.89**	**14.76**	**1999.20**

Table 7 Change detection/transition analysis (2003-2013)

Change detection 2013-2023							
LULC classes		2023					
		Agriculture	Barren Land	Built Up	Mining Area	Water Body	Grand Total
2013	Agriculture	1170.09	127.31	80.20	0.35	0.76	**1378.71**
	Barren Land	82.43	235.74	28.08	0.64	0.58	**347.46**
	Built Up	4.26	2.45	218.15	0.23	0.19	**225.27**
	Mining Area	0.01	0.04	0.02	32.82	0.01	**32.89**
	Water Body	0.05	0.05	0.03	0.00	14.63	**14.76**
	Grand Total	**1256.84**	**365.59**	**326.46**	**34.03**	**16.17**	**1999.10**

Table 8 Change detection/transition analysis (2013-2023)

The change detection matrices in **Table 6, 7 and 8** reveal substantial land transformations over the three decades. Agricultural land declined steadily, with over 200 sq. km converted mainly to built-up and barren categories between 1993 and 2023. Built-up areas expanded rapidly, gaining more than 100 sq. km during 2003–2013, indicating accelerated urban growth. Mining land increased sharply by over 21 sq. km between 2003 and 2013, reflecting intensified extraction before stabilizing thereafter. Overall, the matrices show a clear shift from agriculture toward urban and resource-oriented land uses.

Fig. 6 shows decadal change-detection maps which clearly depicts spatial transitions in Jodhpur Tehsil across the study periods. Agricultural land was progressively converted to built-up and barren areas, particularly in the central and eastern zones. Mining expansion is evident during 2003–2013

and 2013–2023, spreading outward from existing extraction sites. Built-up areas expanded continuously, reflecting rapid urban growth and infilling of former agricultural land. By 2023–2033, intensified shifts toward built-up and mining categories highlight strong anthropogenic pressure on the landscape.

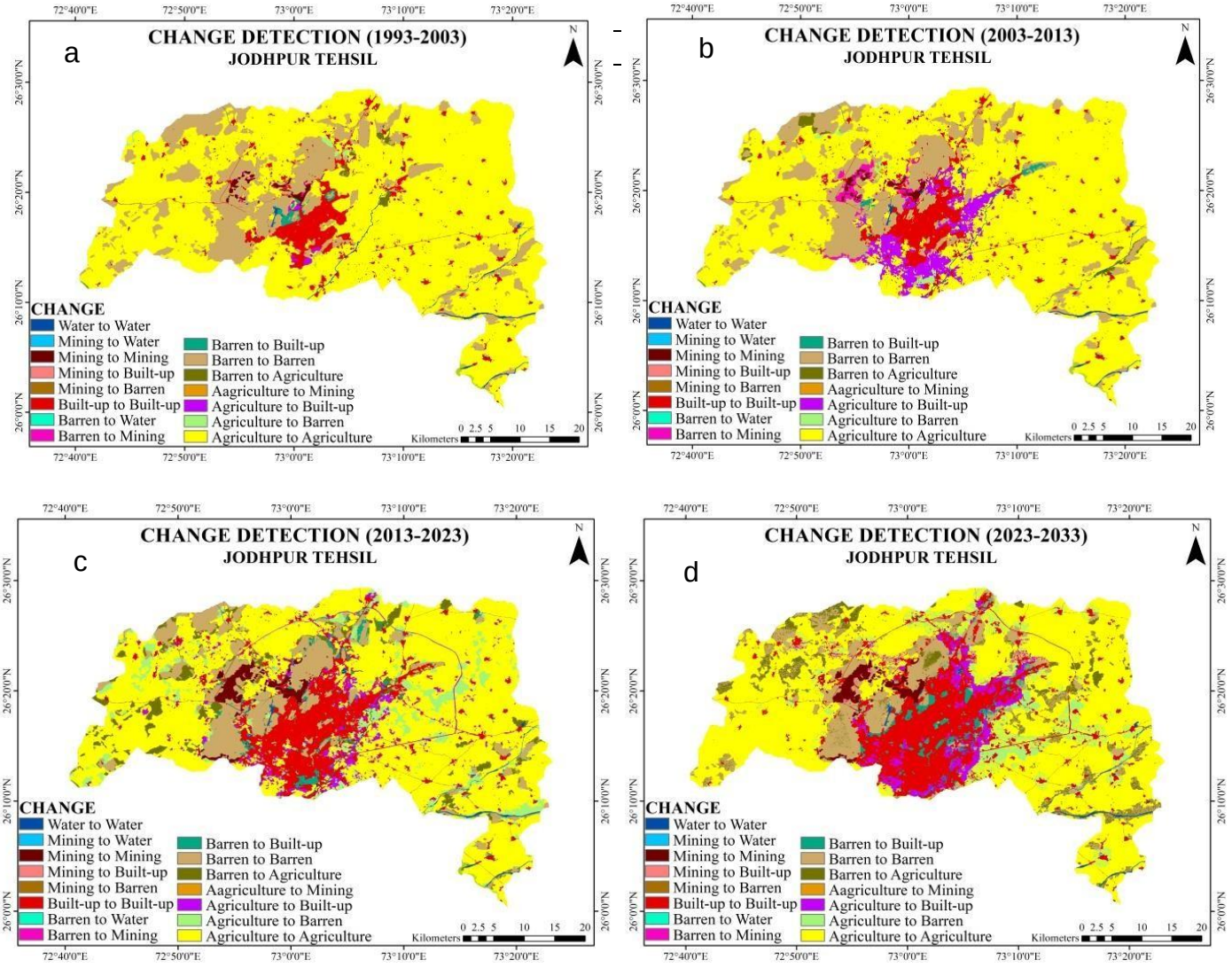

Figure 6 Change detection of LULC, (a) shows change in LULC class during 1993-2003, (b) shows change inLULC class during2003-2013, (c) shows change in LULC during 2013-2023 and (d) shows change in LULCclass during 2013-2023

Table 9 Transition probability matrix (1993-2003)

	Water	Agriculture	Mining	Built-up	Barren
Water	1.000	0.0000	0.0000	0.0000	0.0000
Agriculture	0.0004	0.9940	0.0000	0.0023	0.0033
Mining	0.0000	0.0000	1.0000	0.0000	0.0000
Built-up	0.0004	0.0123	0.0000	0.9867	0.0006
Barren	0.0004	0.0204	0.0053	0.0170	0.9569

Transition 2003-2013					
	Water	**Agriculture**	**Mining**	**Built-up**	**Barren**
Water	0.9942	0.0004	0.0000	0.0054	0.0000
Agriculture	0.0010	0.9317	0.0006	0.0607	0.0060
Mining	0.0023	0.0169	0.9435	0.0128	0.0245

Built-up	0.0000	0.0000	0.0000	1.0000	0.0000
Barren	0.0000	0.0289	0.0562	0.0120	0.9029

Table 10 Transition probability matrix (2003-2013)

Transition 2013-2023					
	Water	**Agriculture**	**Mining**	**Built-up**	**Barren**
Water	0.9334	0.0212	0.0001	0.0114	0.0339
Agriculture	0.0009	0.8478	0.0003	0.0587	0.0923
Mining	0.0003	0.0010	0.9894	0.0028	0.0064
Built-up	0.0013	0.0211	0.0011	0.9649	0.0116
Barren	0.0024	0.2367	0.0021	0.0814	0.6775

Table 11 Transition probability matrix (2013-2023)

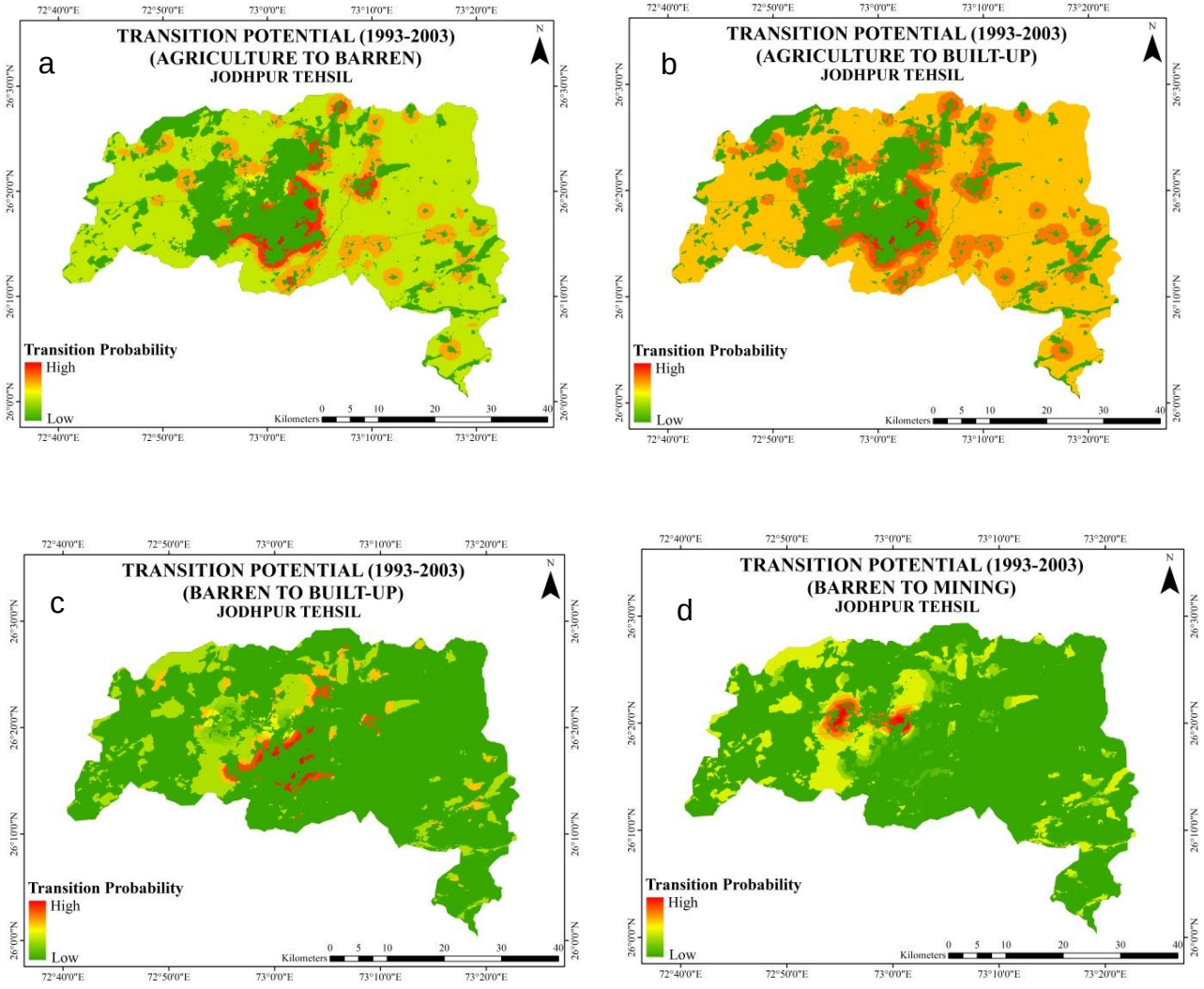

Fig. 7 Maps showing location of low and high transitionpotential during 1993-2003, (a) shows transitionfrom agriculture to barren, (b) shows transition fromagriculture to built-up, (c) shows transition from barren tobuilt-up and (d) shows transition from barren to mining

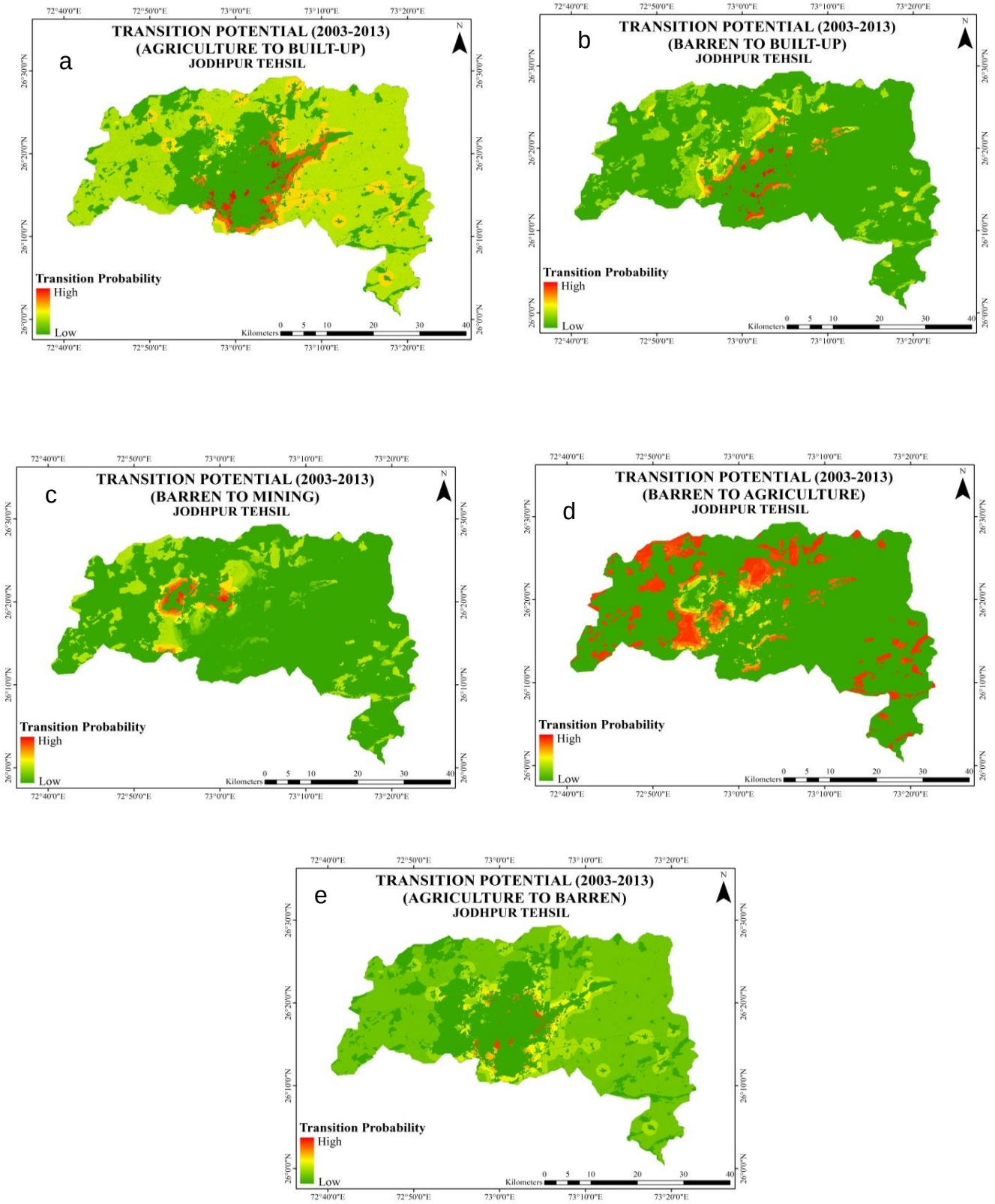

Fig. 8 Maps showing location of low and high transition potential during 2003-2013, (a) shows transitionfrom agriculture to built-up, (b) shows transition from barren to built-up, (c)shows transitionfrom barren tomining, (d) shows transition from barren to agriculture and(e) show transition from agriculture to barren.

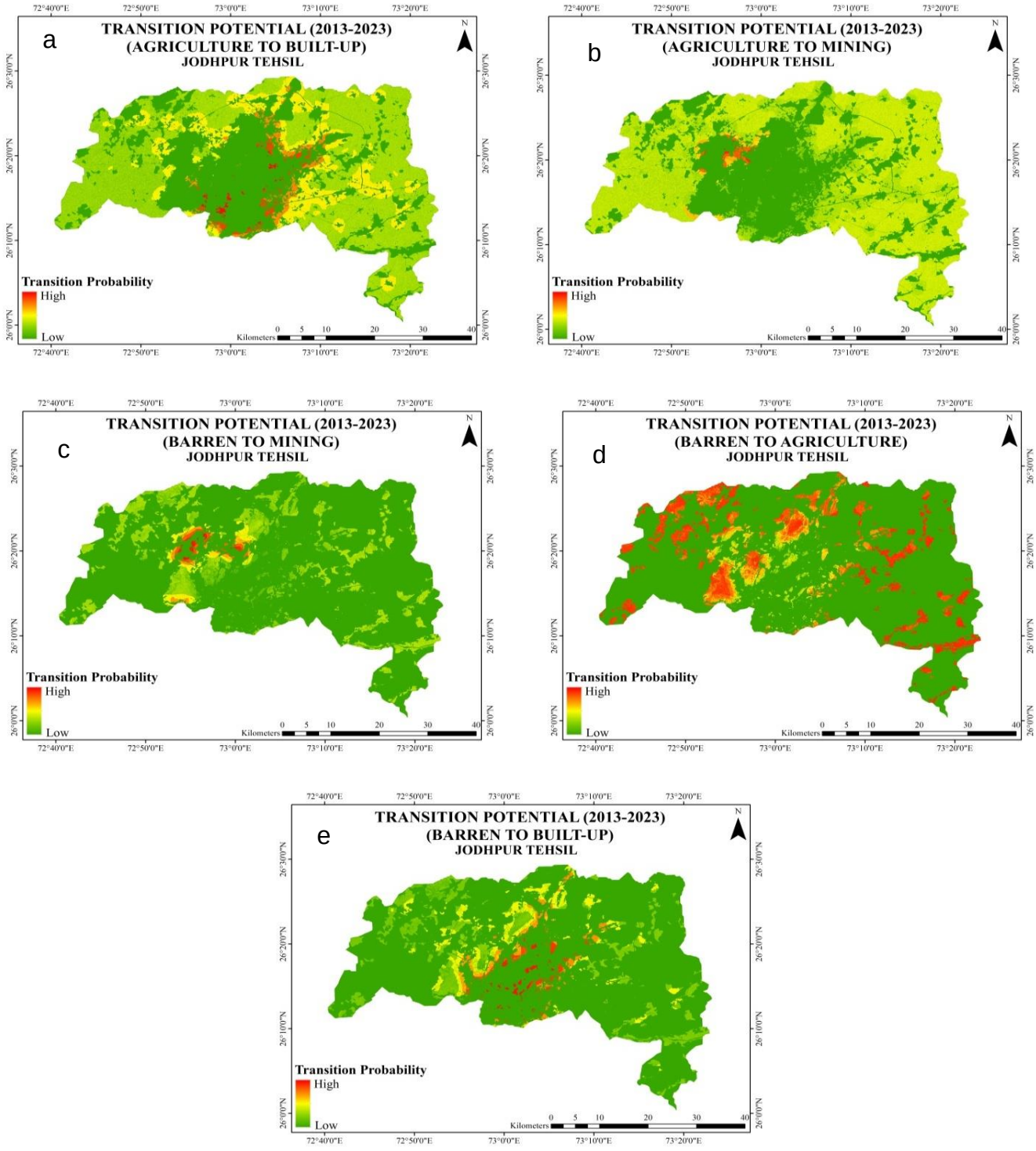

Figure 9 Maps showing location of low and high transition potentialduring 2013-2023, (a) shows transitionfrom agriculture to built-up, (b) shows transition from agriculture to mining, (c) shows transition from barren tomining, (d) shows transition between barren to agriculture and (e) shows transition from barren to built-up

The Transition Probability Matrix (TPM) quantifies the likelihood of LULC changes over time, with values ranging from 0 (no transition) to 1 (complete transition). Rows represent the initial LULC classes, columns indicate the subsequent classes, and diagonal elements show persistence, while off-diagonal values indicate transitions between classes (e.g., agriculture to built-up). The TPM effectively captures landscape dynamics by identifying stable land categories and major patterns of land conversion over time.

The transition probability matrices in **Tables 9, 10, and 11** show clear trends in LULC stability and change over three decades. Agricultural land persistence declined from 0.994 (1993–2003) to 0.848

(2013–2023), reflecting increased conversion to built-up and barren areas. Built-up areas remained highly stable (≥0.96) and increasingly attracted land from agriculture and barren classes. Mining maintained strong persistence (>0.94) but saw growing inflow from barren and agricultural land post-2003, indicating intensified extraction. Barren land transitions rose in 2013–2023, with more land converting to agriculture and built-up, highlighting both degradation and reclamation processes.
The transition-potential maps for 1993-2003 **in Fig 7** 2003-2013, **in Fig 8** and 2013-2023 **in Fig 9** highlight spatial hotspots where agriculture and barren land were most susceptible to conversion into built-up and mining classes. High-probability zones, shown in red, cluster mainly around transport corridors and peri-urban pockets, indicating early phases of urban expansion. Agriculture exhibits strong vulnerability toward both barren and built-up transitions, while barren land shows concentrated potential for mining development.

3.5 Land Use Land Cover Prediction and validation

Validation statistics of predicted LULC (2013 & 2023)		
Validation parameters	**Accuracy 2013 prediction**	**Accuracy 2023 prediction**
Agreement chance	0.1667	0.1667
Agreement quantity	0.2238	0.2037
Agreement grid cell	0.5716	0.5376
Disagree grid cell	0.0120	0.0782
Disagree quantity	0.0260	0.0139
Kno	0.9544	0.8895
Klocation	0.9794	0.8730
KlocationStrata	0.9794	0.8730
Kstandard	0.9377	0.8538

Table 12 Statistics of validation parameter for predicted LULC (2013 & 2023)

Predicted and actual area under each LULC class (2013 & 2023)								
	Actual 2013		**Predicted 2013**		**Actual 2023**		**Predicted 2023**	
	km²	**Percent**	**km²**	**Percent**	**km²**	**Percent**	**km²**	**Percent**
Water	14.76	0.73	14.04	0.70	16.12	0.80	15.97	0.80
Agriculture	1377.82	68.96	1468.06	73.51	1255	62.83	1293.31	64.78
Mining	32.91	1.64	13.58	0.68	33.95	1.69	51.45	2.58
Built-up	225.26	11.27	139.02	6.96	326.75	16.35	312.66	15.66
Barren	347.22	17.37	363.21	18.18	365.54	18.30	323.03	16.18

Table 13 Predicted and actual area under each LULC class (2013-2023)

The LULC prediction and validation process evaluates future land dynamics based on historical transitions and influencing factors. Using the Cellular Automata–Markov Chain (CA–MC) model, future LULC scenarios were simulated, and model-generated maps for 2013 and 2023 were validated against reference data to assess prediction accuracy. Validation employed statistical indices such as agreement measures and Kappa coefficients, ensuring the reliability and robustness of the model. High accuracy in both years indicates strong predictive performance, with a minor decline in precision observed for 2023.
Table 12 presents the statistical validation parameters used to assess the accuracy of LULC predictions for the years 2013 and 2023. The indices, including agreement measures and Kappa coefficients, evaluate how closely the predicted maps align with the reference data.
Overall, the model shows high reliability, with *Kno* (0.9544 for 2013 and 0.8895 for 2023) and *Kstandard* (0.9377 for 2013 and 0.8538 for 2023) indicating strong predictive performance, though a slight decline in accuracy is observed for 2023.

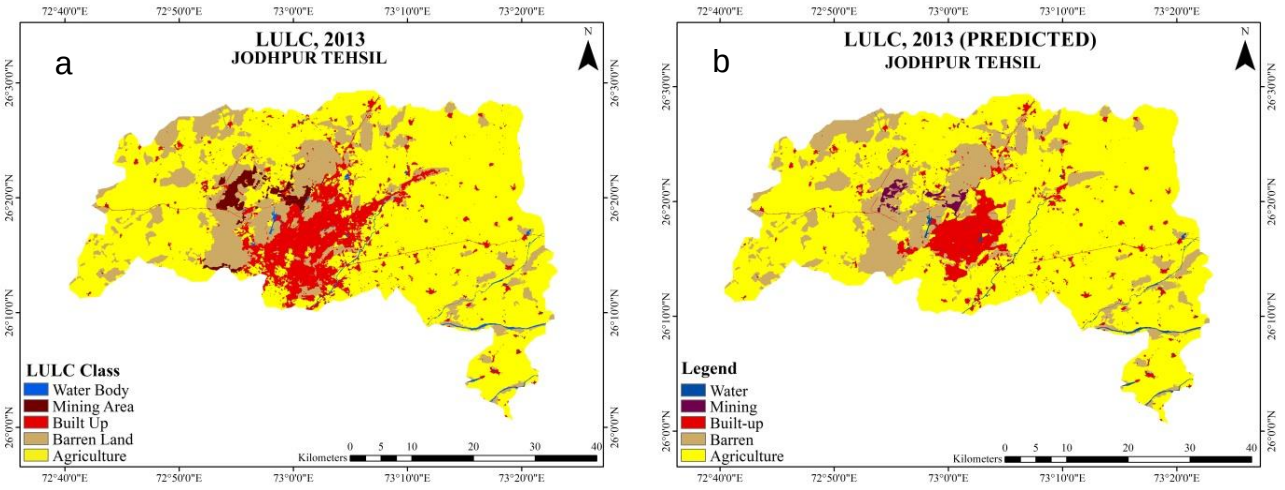

Figure10: Comparison between actual and predicted LULC, (a) shows actual LULC of 2013 and (b) shows predicted LULC of 2013

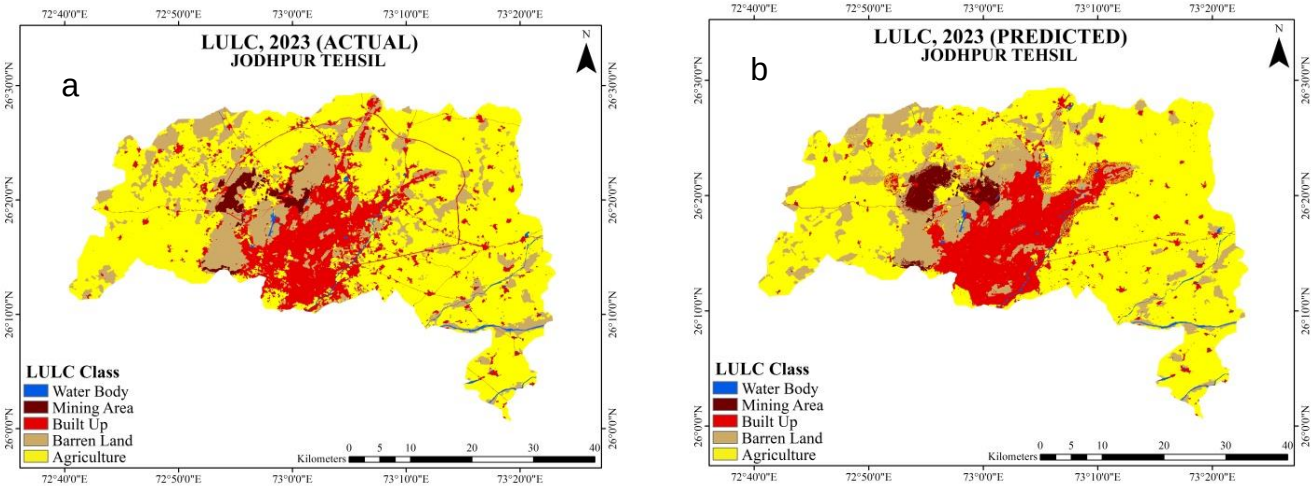

Figure 11: Comparison between actual and predicted LULC, (a) shows actual LULC of 2023 and (b) shows predicted LULC of 2023

According to **Table 13**, the comparison between actual and predicted 2013 LULC **in Fig. 10** revealsstrong agreement for major classes such as water, agriculture, and barren land. The model slightlyoverestimates agricultural area while underestimating mining and built-up categories. Overall, **Table11** reflects a generally accurate prediction performance with only minor class-wise discrepancies.

Table 13 and **Fig. 11** compares the actual and model-predicted LULC areas for 2023 across major classes. The results indicate close alignment between observed and simulated values, reflecting strong model accuracy. Minor variations, such as a slight increase in predicted agricultural and mining areas, suggest ongoing land transformation trends.

Predicted LULC area		
	Predicted 2033	
	Km^2	**Percentage**
Water	17.17	0.86

Agriculture	1159.95	58.10
Mining	35.04	1.76
Built-up	418.37	20.96
Barren	365.85	18.33

Table 14 Predicted area under each LULC class (2033)

Fig. 12(a) presents the projected LULC map for Jodhpur Tehsil in 2033, indicating major landscapetransformations. Built-up areas show substantial expansion, predominantly in the central and easternregions, reflecting intensified urban growth. Agricultural land continues to dominate but displaysnoticeable fragmentation due to increasing mining and urban activities. Overall, **Fig. 12** highlightssignificant shifts driven by development pressure and changing land-use dynamics.
Table 14 presents the projected LULC distribution for 2033, highlighting expected spatial changes across major land categories. The model predicts a noticeable rise in built-up areas alongside a decline in agricultural land, indicating continued urban expansion. Water, mining, and barren land show relatively stable proportions, suggesting moderate landscape transformation by 2033.

Predicted change detection 2023-2033							
LULC CLASSES		**2033**					
		Agriculture	**Barren Land**	**Built Up**	**Mining Area**	**Water Body**	**Grand Total**
2023	**Agriculture**	1056.03	115.78	80.33	0.42	2.01	1254.57
	Barren Land	89.14	239.99	32.99	1.34	1.67	365.13
	Built Up	13.13	8.02	303.57	0.56	0.97	326.26
	Mining Area	0.16	0.79	0.35	32.71	0.02	34.02
	Water Body	1.23	1.26	1.14	0.02	12.49	16.14
	Grand Total	**1159.70**	**365.83**	**418.37**	**35.05**	**17.17**	**1996.11**

Table 15 Predicted change detection analysis (2023-2033)

Fig. 12(b) illustrates the projected land use/land cover changes in Jodhpur Tehsil for 2023–2033,highlighting significant transitions across the region. Large areas are expected to convert fromagriculture and barren land to built-up and mining classes, indicating intensified urbanization andresource extraction. The spatial distribution in **Fig. 12** also reveals fragmented patches of agriculturalrecovery and localized shifts from mining and barren classes to more productive land uses.
Table 15 illustrates the predicted LULC transitions between 2023 and 2033. The dominant trend is the conversion of agricultural land to built-up areas (80.33 km²), emphasizing ongoing urbanization. Barren land and agricultural conversions also persist, while mining and water bodies remain relatively stable.
The validation and prediction results confirm that the CA–Markov model provides a robust representation of land transformation trends within the study area. Agricultural land continues to decline steadily, primarily converting to built-up and barren areas, reflecting rapid urbanization and infrastructure expansion. The 2033 prediction indicates further intensification of urban growth at the expense of agricultural land, underscoring the need for sustainable land management strategies to balance development and environmental conservation.

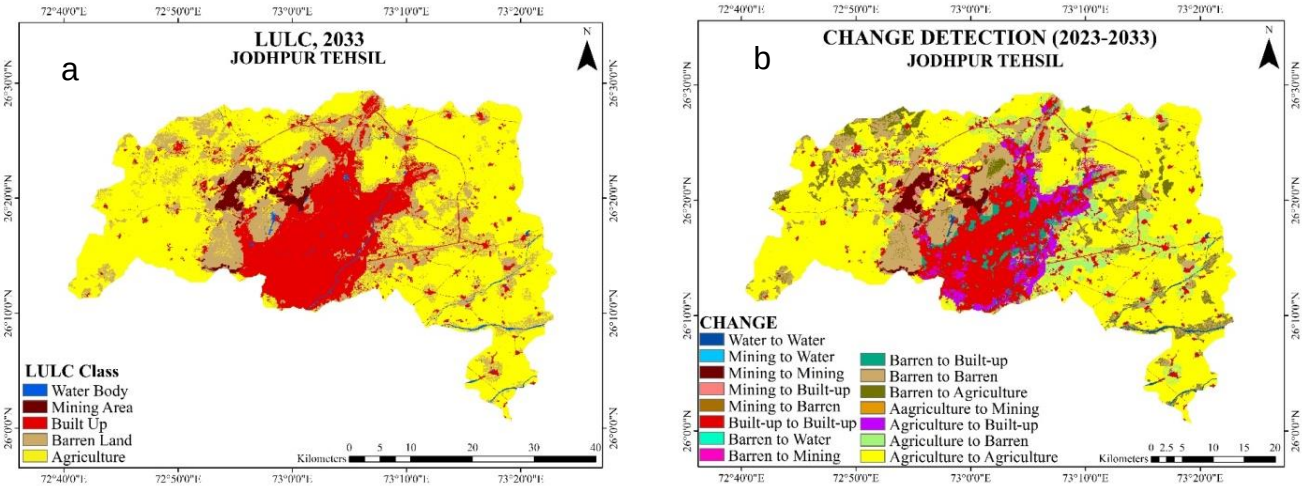

Figure 12: LULC Prediction, (a) shows predicted LULC of 2033 and (b)showspredicted change in LULCduring 2023-2033

Conclusion

This study examined the spatial and temporal changes in Land Use and Land Cover (LULC) in Jodhpur Tehsil, Rajasthan, from 1993 to 2023 and projected future patterns for 2033 using the CA–Markov model in the TerrSet system. Analysis of multi-decadal Landsat imagery shows a clear human-driven transformation of the landscape, marked by a steady reduction in agricultural land and a rapid increase in built-up and mining areas. These changes reflect growing urbanization, infrastructure expansion, and resource extraction in the region.

Model validation demonstrated strong agreement between observed and predicted maps, confirming the reliability of the CA–Markov approach for simulating future land transitions. The transition analysis indicates that agricultural and barren lands are increasingly vulnerable to conversion into urban and mining uses, suggesting continued pressure on land resources.

Overall, the findings highlight rising anthropogenic stress on Jodhpur's fragile arid environment and emphasize the need for informed land-use planning to balance development with environmental sustainability.

Conflict of interest

The authors have no competing interests to declare that are relevant to the content of this article.

Data Availability Statement

No

References

1. Parveen, S., Basheer, J., & Praveen, B. (2018). A literature review on land use land cover changes. *International Journal of Advanced Research*, *6*(7), 1-6. **DOI URL:** https://dx.doi.org/10.21474/IJAR01/7327
2. von Keyserlingk, J., Thieken, A. H., & Paton, E. N. (2023). Approaches to assess land degradation risk:a synthesis. *Ecology and Society*, *28*(1).
3. Thakur, T. K., Swamy, S. L., Dutta, J., Thakur, A., Mishra, A., Sarangi, P. K., Kumar, A., Almutairi, B. O., & Kumar, R. (2024). Assessment of land use dynamics and vulnerability to land degradation in coal-mined landscapes of central India: Implications for ecorestoration strategies. *Frontiers in Environmental Science*, *12*, 1419041.**DOI URL:** https://doi.org/10.3389/fenvs.2024.1419041

4. Nath, B., Wang, Z., Ge, Y., Islam, K., P. Singh, R., & Niu, Z. (2020). Land use and land cover change modeling and future potential landscape risk assessment using Markov-CA model and analytical hierarchy process. *ISPRS International Journal of Geo-Information*, *9*(2), 134.
5. Taloor, A. K., Sharma, S., Parsad, G., & Jasrotia, R. (2024). Land use land cover simulations using integrated CA-Markov model in the Tawi Basin of Jammu and Kashmir India. *Geosystems and Geoenvironment*, *3*(2), 100268.
6. Tiamgne, X. T., Kalaba, F. K., & Nyirenda, V. R. (2022). Mining and socio-ecological systems: A systematic review of Sub-Saharan Africa. *Resources policy*, *78*, 102947. **DOI URL** :https://doi.org/10.1016/j.resourpol.2022.102947
7. da Cunha, E. R., Santos, C. A. G., da Silva, R. M., Bacani, V. M., & Pott, A. (2021). Future scenarios based on a CA-Markov land use and land cover simulation model for a tropical humid basin in the Cerrado/Atlantic forest ecotone of Brazil. *Land Use Policy*, *101*, 105141.**DOI URL** : https://doi.org/10.1016/j.jenvman.2020.111706
8. Mwabumba, M., Yadav, B. K., Rwiza, M. J., Larbi, I., & Twisa, S. (2022). Current Research in Environmental Sustainability. *Current Research in Environmental Sustainability*, *4*, 100126.
9. Surabuddin Mondal, M., Sharma, N., Kappas, M., & Garg, P. K. (2019). Ca Markov modeling of land use land cover dynamics and sensitivity analysis to identify sensitive parameter (S). *The International Archives of the Photogrammetry, Remote Sensing and Spatial Information Sciences*, *42*, 723-729.**DOI URL** : https://doi.org/10.5194/isprs-archives-XLII-2-W13-723-2019
10. Sisay, G., Gessesse, B., Fürst, C., Kassie, M., & Kebede, B. (2023). Modeling of land use/land cover dynamics using artificial neural network and cellular automata Markov chain algorithms in Goang watershed, Ethiopia. *Heliyon*, *9*(9).
11. Aksoy, H., & Kaptan, S. (2022). Simulation of future forest and land use/cover changes (2019–2039) using the cellular automata-Markov model. *Geocarto International*, *37*(4), 1183-1202. **DOI URL** : https://doi.org/10.1080/10106049.2020.1778102
12. Saharan, M. A., Vyas, N., Borana, S. L., & Yadav, S. K. (2018). Classification and assessment of the land use–land cover changes in Jodhpur City using remote sensing technologies. *The International Archives of the Photogrammetry, Remote Sensing and Spatial Information Sciences*, *42*, 767-771. **DOI URL** : https://doi.org/10.5194/isprs-archives-XLII-5-767-2018
13. Borana, S. L., Yadav, S. K., & Parihar, S. K. (2017). Spatio-temporal assessment of vegetation cover of Jodhpur city and surrounding areas. *International Journal of Innovative Research in Computerand Communication Engineering*, *5*(10).
14. Ground Water Department, Government of Rajasthan. (2018) *Rajasthan Ground Water Vision Report.* Jaipur: Government of Rajasthan.**DOI URL** : 10.22271/allresearch.2025.v11.i1e.12310
15. Arsanjani, J. J., Helbich, M., Kainz, W., & Boloorani, A. D. (2013). Integration of logistic regression, Markov chain and cellular automata models to simulate urban expansion. *International Journal of Applied Earth Observation and Geoinformation*, *21*, 265-275.**DOI URL** : https://doi.org/10.1016/j.jag.2011.12.014
16. Pontius Jr, R. G., Huffaker, D., & Denman, K. (2004). Useful techniques of validation for spatially explicit land-change models. *Ecological modelling*, *179*(4), 445-461. **DOI URL** : https://doi.org/10.1016/j.ecolmodel.2004.05.010
17. Congalton, R. G., & Green, K. (2019). *Assessing the accuracy of remotely sensed data: principles and practices*. CRC press. **DOI URL** :https://doi.org/10.1201/9780429052729
18. Pontius Jr, R. G., Boersma, W., Castella, J. C., Clarke, K., de Nijs, T., Dietzel, C., ... & Verburg, P. H. (2008). Comparing the input, output, and validation maps for several models of land change. *The annals of regional science*, *42*(1), 11-37. **DOI URL** : https://doi.org/10.1016/j.jag.2011.12.014
19. Sang, L., Zhang, C., Yang, J., Zhu, D., & Yun, W. (2011). Simulation of land use spatial pattern of towns and villages based on CA–Markov model. *Mathematical and Computer Modelling*, *54*(3-4), 938943. **DOI URL** : https://doi.org/10.1016/j.mcm.2010.11.019

20. Mas, J. F., Kolb, M., Paegelow, M., Olmedo, M. T. C., & Houet, T. (2014). Inductive pattern-based land use/cover change models: A comparison of four software packages. *Environmental Modelling & Software*, *51*, 94-111. **DOI URL** : https://doi.org/10.1016/j.envsoft.2013.09.010
21. Guan, D., Li, H., Inohae, T., Su, W., Nagaie, T., & Hokao, K. (2011). Modeling urban land use change by the integration of cellular automaton and Markov model. *Ecological modelling*, *222*(20-22), 37613772. **DOI URL** : https://doi.org/10.1016/j.ecolmodel.2011.09.009
22. Pontius Jr, R. G., & Millones, M. (2011). Death to Kappa: birth of quantity disagreement and allocation disagreement for accuracy assessment. *International journal of remote sensing*, *32*(15), 4407-4429. **DOI URL** : https://doi.org/10.1080/01431161.2011.552923
23. Pontius Jr, R. G., Boersma, W., Castella, J. C., Clarke, K., de Nijs, T., Dietzel, C., ... & Verburg, P. H. (2008). Comparing the input, output, and validation maps for several models of land change. *The annals of regional science*, *42*(1), 11-37. **DOI URL** : https://doi.org/10.1007/s00168-007-0138-2
24. Landis, J. R., & Koch, G. G. (1977). The measurement of observer agreement for categorical data. *biometrics*, 159-174.**DOI URL** : https://doi.org/10.2307/2529310